# Tensile and Compressive Behavior of Poly(*p*-phenylene benzobisthiazole) Fibers

MOHSEN SAHAFEYAN and SATISH KUMAR*

School of Textile and Fiber Engineering, Georgia Institute of Technology, Atlanta, Georgia 30332

SYNOPSIS

Heat treated poly(*p*-phenylene benzobisthiazole) (PBZT) fibers tested in tension result in two types of failure modes. In failure mode I, the fiber exhibits a relatively sharp break; mode II is characterized by significant axial fiber splitting. Approximately 20% of the fibers failed in mode II when tested at 2.54, 7.62, and 12.7 cm gage lengths. At 1.25 cm gage length all the fibers failed in mode I. Tensile strength decreased from the 1.25 to 7.62 cm gage length, but tensile strength of the fibers tested at 7.62 and 12.7 cm gage lengths were similar. The two failure mode observation is supported by the Weibull statistical distribution. Fiber tensile properties were also measured at 150°C. Axial compressive strength of the PBZT fibers as determined from the recoil test is also reported and is found to be independent of fiber tensile modulus and fiber diameter. As-received heat-treated fibers were post heat treated between 700 and 775°C. Structural changes in the fiber were studied using infrared spectroscopy, small and wide angle x-ray scattering, and swelling studies. © 1995 John Wiley & Sons, Inc.

## INTRODUCTION

Poly(*p*-phenylene benzobisthiazole) (PBZT) is a rigid-rod molecule characterized with high thermal stability (onset of thermal degradation in air > 600°C), high chain stiffness (theoretical chain modulus is predicted to be close to 700 GPa), and high radiation resistance. The PBZT fibers are directly spun from the polymerization solution in poly(phosphoric acid) at a typical polymer molecular weight of 25,000 g/mol at about 15 wt % in solution using a dry jet wet spinning technique. The fibers are generally coagulated in water at room temperature, dried, and subsequently heat treated under tension for 1–2 min in the temperature range of 550–700°C. The polymer spinning solution is characterized as a nematic liquid crystal. In addition to their dissolution in strong protic solvents, polymers such as PBZT can also be dissolved in nitroalkanes (e.g. nitromethane) where solubilization is mediated via a Lewis acid (e.g. $AlCl_3$).[1] The science and engineering of rigid-rod polymers, including PBZT fibers, has been reviewed.[2-4] In an attempt to influence the fiber compressive strength, various chemical modifications of the PBZT molecule have been reported.[2,4] However to date the maximum compressive strength of polymeric materials is limited to about 500 MPa; the compressive strength of various carbon fibers range from 0.5 GPa to about 3.0 GPa. For inorganic fibers such as alumina (> 95% $Al_2O_3$) and boron fibers, compressive strength values as high as 7 GPa have been reported. Various issues related to compressive strength of glassy resins, high performance polymeric and carbon fibers, and polymeric matrix composites have recently been addressed.[5-7] In this article we report the axial tensile and compressive behavior of heat-treated PBZT fibers.

## EXPERIMENTAL

Multifilament heat-treated PBZT fibers were received from the Air Force Materials Laboratory. The properties of one as-received fiber referred to as fiber F are given in Table I. The single fibers separated from the multifilament bundle were mounted on

* To whom correspondence should be addressed.

Journal of Applied Polymer Science, Vol. 56, 517–526 (1995)
 CCC 0021-8995/95/040517-10

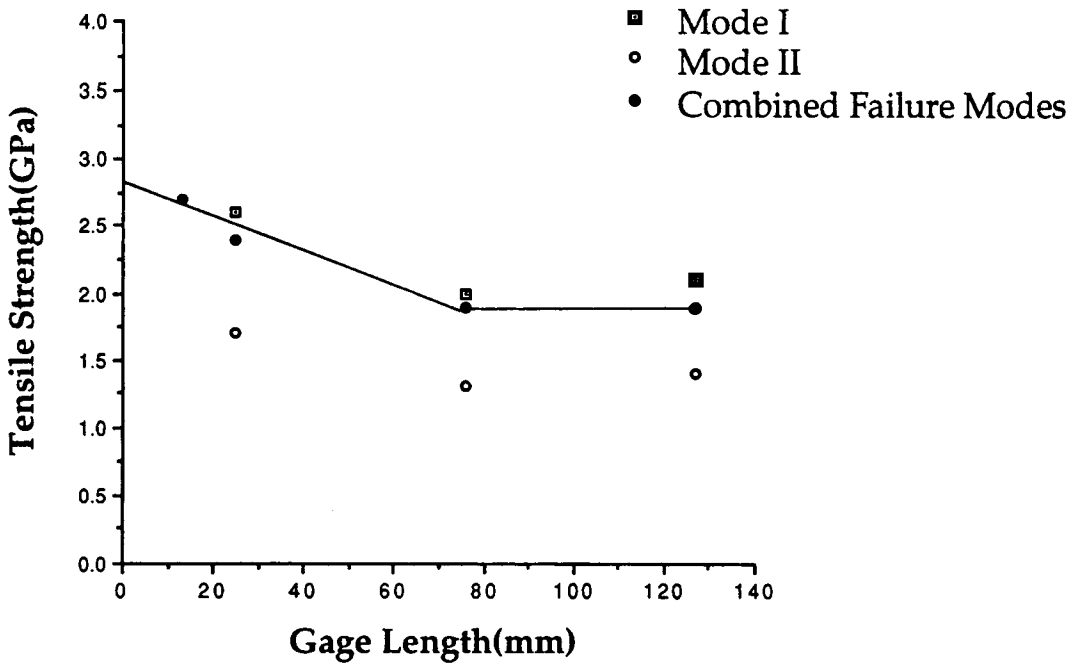


**Figure 1** Tensile strength of PBZT fiber F as a function of gage length.

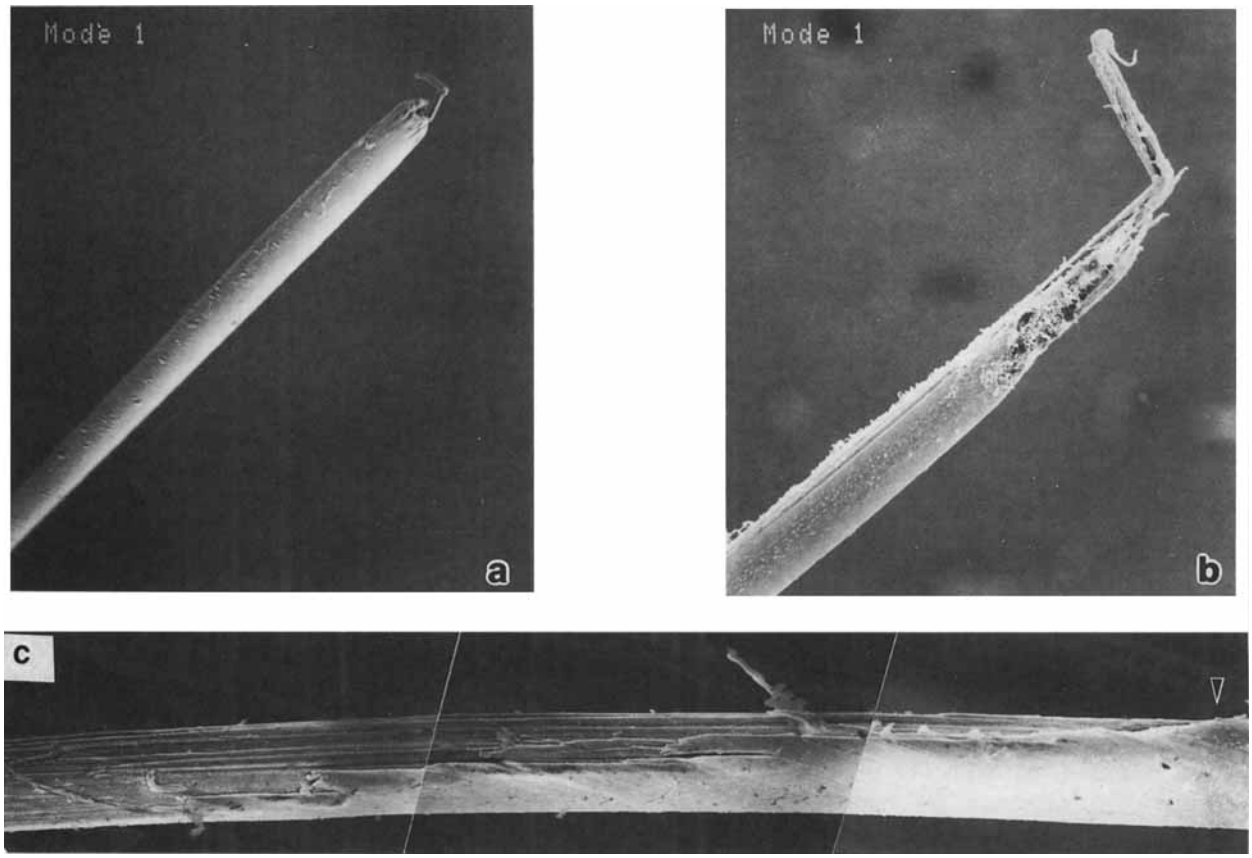


**Figure 2** Scanning electron micrographs of tension fractured PBZT fiber F. (a) and (b) failure mode I, (c) failure mode II. Fiber diameter 16 $\mu$m.

**Table I Properties of Heat-Treated PBZT Fiber (Fiber F)**

| | |
|---|---|
| Diameter ($\mu$m) | 16.1 ± 0.6 |
| Recoil compressive strength (GPa) | 0.28 ± 0.02 |
| Tensile modulus (GPa)[a] | 210 ± 20 (at 2.54 cm) |
| Tensile strength (GPa)[b] | 2.4 ± 0.5 (at 2.54 cm) |
| Density (gm/cm$^3$) | 1.61 ± 0.01 |

[a] Machine compliance corrected modulus 250 GPa.
[b] 2.9 GPa at zero gage length.

precut paper tabs using scotch tape and Loctite™ glue. Tensile stress–strain experiments were conducted on an Instron tensile tester model 1125 at 1.25, 2.54, 7.62, and 12.7 cm gage lengths at crosshead speed of 0.05 cm/min. Approximately 100 samples were tested at each gage length. The fractured fiber ends were observed with a magnifying glass for identification of the fracture mode. Representative samples of the two failure modes were also examined in the scanning electron microscope (Hitachi S-800). Tensile strength values were calculated for each failure mode.

Compressive strength of the samples was measured using the recoil test at 2.54 cm gage length.[8–10] Electric spark was used for cutting the samples.[11] Fiber diameter was measured using the laser diffraction technique.[12] Fibers were post heat treated at 725, 750, and 775°C in nitrogen atmosphere for 30 s without tension in a horizontal Lindberg furnace. Swelling studies on the as-received and post heat-treated fibers were carried out in 85% methane sulfonic acid by monitoring the fiber diameter using the laser diffraction technique. Wide-angle x-ray diffraction was carried out on a four-circle diffractometer using Cu K$\alpha$ radiation from a Rigaku RU-200 rotating anode generator.

Weakest link theory[13] states that fibers of length $nl$ have the same strength distribution as $n$ fibers of length $l$. Mathematically this can be stated as:

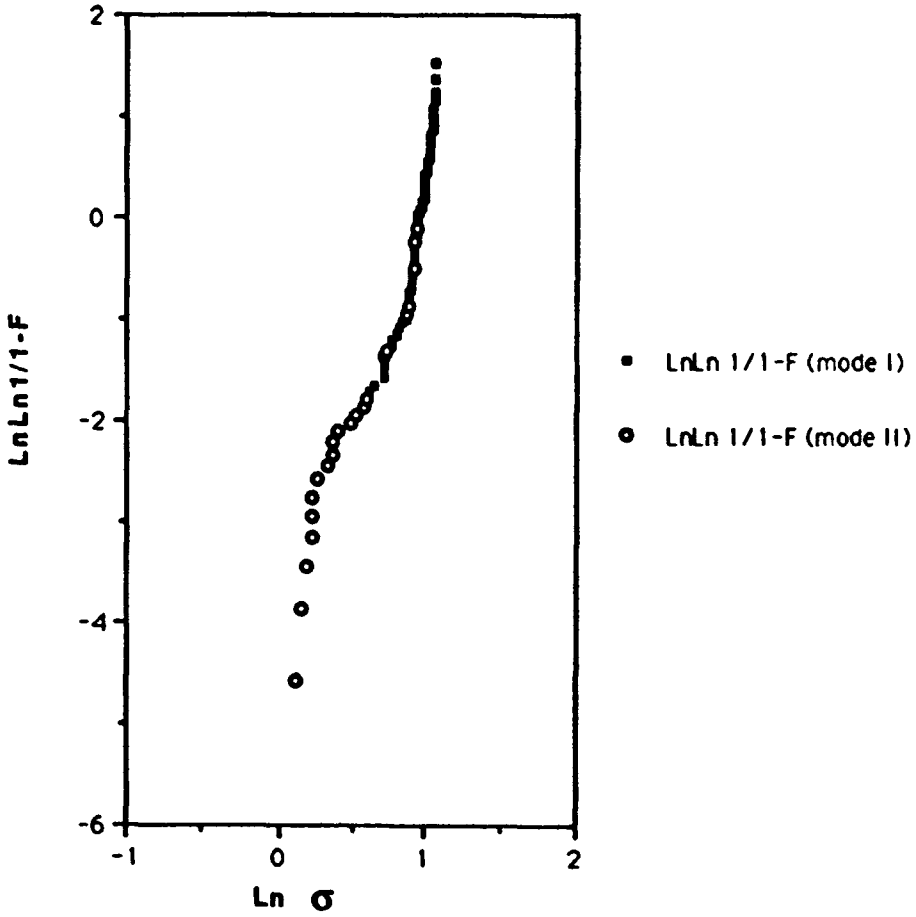


**Figure 3** Linearized Weibull plot of PBZT fiber F at 2.54 cm gage length. $\sigma$ is tensile stress at failure in GPa.

$$1 - F_{nl}(\sigma) = [1 - F_l(\sigma)]^n \quad (1)$$

where $F_{nl}(\sigma)$ and $F_l(\sigma)$ are cumulative failure probabilities at stress $\sigma$ for fibers of length $nl$ and $l$, respectively. According to the Weibull distribution, the cumulative failure probability of a fiber of length $l$ at stress $\sigma$ is

$$F = 1 - \exp[-l(\sigma/\sigma_0)^m] \quad (2)$$

where $m$ and $\sigma_0$ are Weibull parameters and are called shape and scale parameters, respectively. The shape parameter $m$ indicates the flaw frequency distribution and $\sigma_0$ is a stress normalizing factor. The Weibull distribution can be written as

$$\ln \ln[1/(1 - F)] = m \ln \sigma + m \ln(l^{1/m}/\sigma_0). \quad (3)$$

A plot of $\ln \ln[1/(1 - F)]$ vs. $\ln \sigma$ yields $m$ and $\sigma_0$.

Beetz[14,15] showed that multimode failure for fibers exhibits as peaks in a histogram of number percent (fraction) of failed fibers vs. tensile strength. The multimode failure also corresponded to a break in the Weibull plot of eq. (3). He hypothesized that there are two type of defects and that each fiber failed by one or the other type of defect. Thus, he could write the survival probability ($P = 1 - F$) for a fiber under load $\sigma$ as a mixed survival probabilities $P_I$ and $P_{II}$ as:

$$P = \alpha P_I + (1 - \alpha)P_{II}. \quad (4)$$

**Table II Weibull Parameters for PBZT Fiber (Fiber F) Failed in Mode I and II**

| | Gage Lengths (mm) | | | | | |
|---|---|---|---|---|---|---|
| | Mode I | | | Mode II | | |
| | 25 | 76 | 125 | 25 | 76 | 125 |
| $\sigma_0$ | 2.9 | 2.9 | 3.2 | 1.6 | 2.2 | 4.1 |
| $m$ | 10.2 | 7.6 | 7.8 | 14.2 | 6.9 | 3.7 |

## RESULTS AND DISCUSSION

The average tensile strength values for each failure mode, and the weighted average tensile strength of the two failure modes are plotted in the Figure 1. At the 1.25 cm gage length, mode II failure was not observed. Tensile failure stress values at 7.6 and 12.7 cm were about the same for both failure modes. Scanning electron micrographs of the two types of

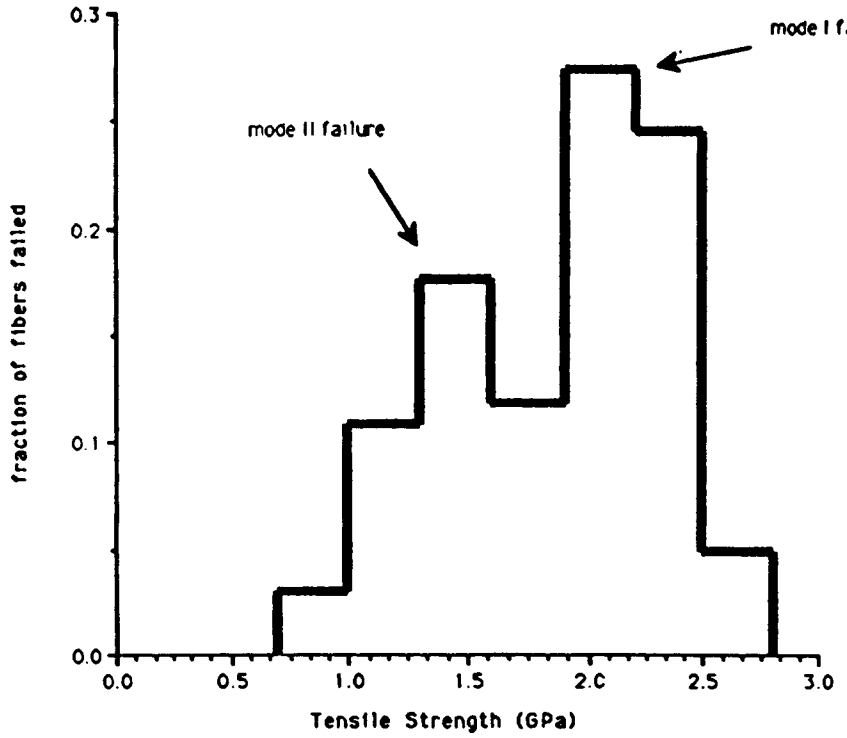


**Figure 4** Tensile strength distribution for PBZT fiber F tested at 7.6 cm gage length.

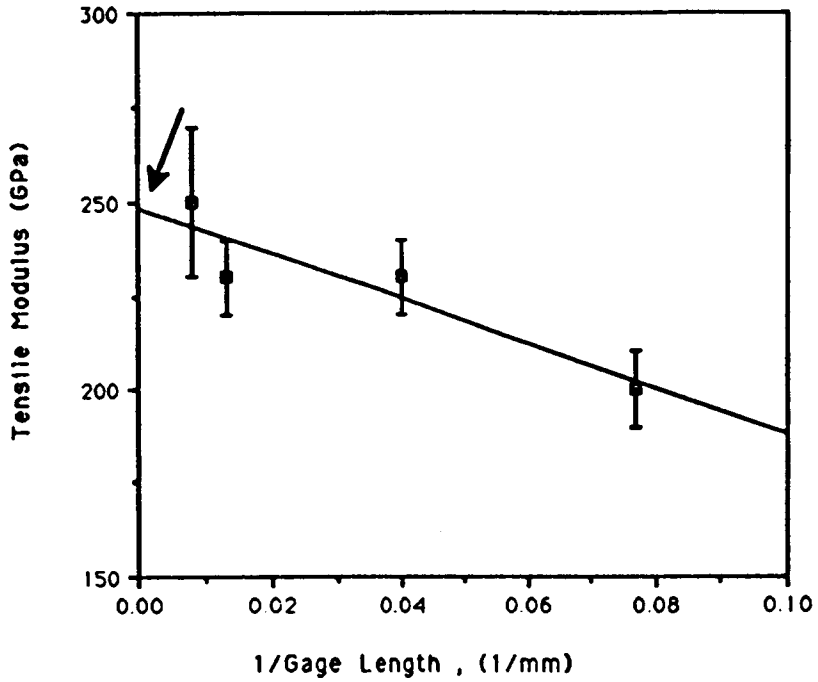


**Figure 5** Tensile modulus of PBZT fiber as a function of 1/gage length. Arrow indicates compliance corrected modulus value.

tensile failure are shown in Figure 2. Figure 2(a,b) show little or no splitting along the fiber axis and little fibrillation. This type of failure where very little or no splitting is observed was referred to as mode I failure. The mode II type failure is shown in Figure 2(c). In this case tensile failure was accompanied with significant fiber splitting running many times the fiber diameter along the length of the fiber. For the particular fiber shown in Figure 2(c) fiber splitting occurred along the 1500 $\mu$m length, or approximately 100 times the fiber diameter. Fiber splitting has also been reported in aramid fibers.[16] Fibers that failed in mode I have significantly higher tensile strength than the fibers that failed in mode II. This result indicates that if fiber processing could be modified to avoid axial fiber splitting during tensile fracture, then average fiber tensile strength could be improved. A slower coagulation process may be helpful in this regard. The number of fibers failed by mode II at 2.54, 7.62, and 12.7 cm gage lengths were 23, 15, and 19%, respectively of the total fibers tested for a particular gage length. The lack of significant fiber splitting (mode II failure) in the 1.25 cm gage length samples is probably a result of reduced probability of finding the initiation points for fiber splitting in the short gage length fibers. The fact that the tensile strength values for 7.62 and 12.7 cm samples are the same suggests that the probability of finding defects that lead to tensile failure has reached 100% in the 7.62 cm sample. Tensile stress–strain curves were also obtained on the PBZT fibers at 150°C using a miniature materials tester from the Polymer Laboratory. Both tensile strength and tensile modulus of the PBZT fiber at the 2.54 cm gage length at 150°C are about 85% of their respective room temperature values.

The linearized Weibull plot of the tensile strength data of the fiber tested at the 2.54 cm gage length is given in Figure 3. In this plot, two distinct regions characterized with two straight lines are observed, which corresponds to two different failure modes. A histogram of the fraction of fibers failed vs. tensile strength for 76 cm gage length fibers is given in Figure 4, which also shows a bimodal distribution. The strength values corresponding to the two peaks are 1.5 and 2.2 GPa, corresponding to the mode II and mode I failures, respectively. The Weibull parameters $\sigma_0$ and $m$ for the two failure modes are given in Table II. The average values of $\sigma_0$ and $m$ for all gage lengths for the failure mode I are 3.0 and 8.5, respectively, and for failure mode II, average $\sigma_0$ and $m$ values are 2.6 and 8.3, respectively.

A plot of tensile modulus as a function of gage length in Figure 5 indicates the effect of machine compliance, and emphasizes either the necessity of making correction for machine compliance or mak-

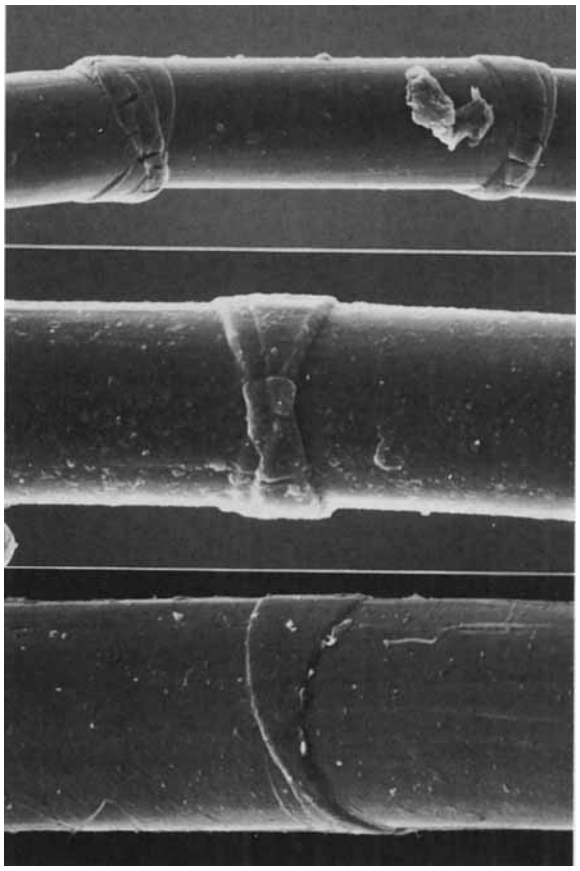

**Figure 6** Scanning electron micrographs of PBZT fibers failed in recoil compression. Fiber diameter 16 $\mu$m.

ing modulus measurements at high gage lengths for high modulus fibers.

For compression testing, fibers were mounted on the precut 2.54 cm gage length paper tabs similar to the tensile specimens. Fibers were stretched to a predetermined stress level and then cut at the center using an electric spark. Both fiber halves were examined for kinks. The type of kinks observed in PBZT fibers during recoil compression are given in Figure 6. All polymeric fibers are known to fail in the kinking manner in compression. Tensile strength of the fiber with a compression kink is about the same as the tensile strength of the unkinked fiber. This suggest that the polymer molecules involved in the kinking process glide past each other and change their orientation at the compressive stress, and that these molecules do not break resulting in a noncatastrophic compression failure. On the other hand, inorganic and carbon fibers generally exhibit catastrophic failure in compression. The typical data obtained from recoil compression is given in Figure 7. The fiber compressive strength has been taken as the stress at 50% failure probability. As-received heat-treated fibers with varying spinning conditions, heat-treatment temperature, and draw ratios have a range of fiber diameters and tensile moduli. Compressive strength of the as-received fibers as a function of tensile modulus and as a function of fiber diameter is presented in Figures 8 and 9. The data in these two figures suggests at best a very moderate increase in fiber compressive strength either with fiber modulus or with fiber diameter. However as the increase is within the measurement error, no meaningful significance is attached to this increase.

In an attempt to further influence the fiber structure and possibly properties such as compressive strength, one of the as-received fibers was further heat treated to 725, 750, and 775°C for approximately 30 s. The compressive strength of these post heat-treated and control fibers is also plotted in Figure 8 as a function of fiber modulus. No significant effect of the post heat treatment was observed on compressive strength. However, the swelling data presented in Figure 10 indicates that the swelling in the control fiber is much higher than in the post heat-treated fiber. The question is whether the lack of swelling in post heat-treated fibers is due to crosslinking or a result of increased order and crystallinity. Fourier transform infrared (FTIR) spectra of the control and that of the post heat-treated samples were identical, and so were the elemental analyses of the two samples. From these, it seems that significant crosslinking did not occur on post heat treatment, leaving the possibility that the swelling differences may arise due to enhanced crystalline order. On post heat treatment, crystallite size measured from wide angle x-ray scattering for the (200) plane increased from 9.8 to 10 nm and for the (010) plane it increased from 5 to 5.3 nm. The crystallite size differences between the control and the post heat-treated fibers are small, however this could possibly explain the swelling data. On post heat treatment the enhancement of order in the fiber may be limited to the fiber surface, preventing or delaying the diffusion of the methane sulfonic acid to the less ordered core where swelling could occur. Although the increase in crystallite size is very small, the volume fraction of the ordered area may have increased significantly. On post heat treatment the layer line becomes sharper. This is clearly evidenced from the second layer line (at $2\theta$ of approximately 14°) intensity comparison between the control and the post heat-treated samples in Figure 11. On post heat treatment, the second layer line separates into more distinct spots, as evidenced from the meridional

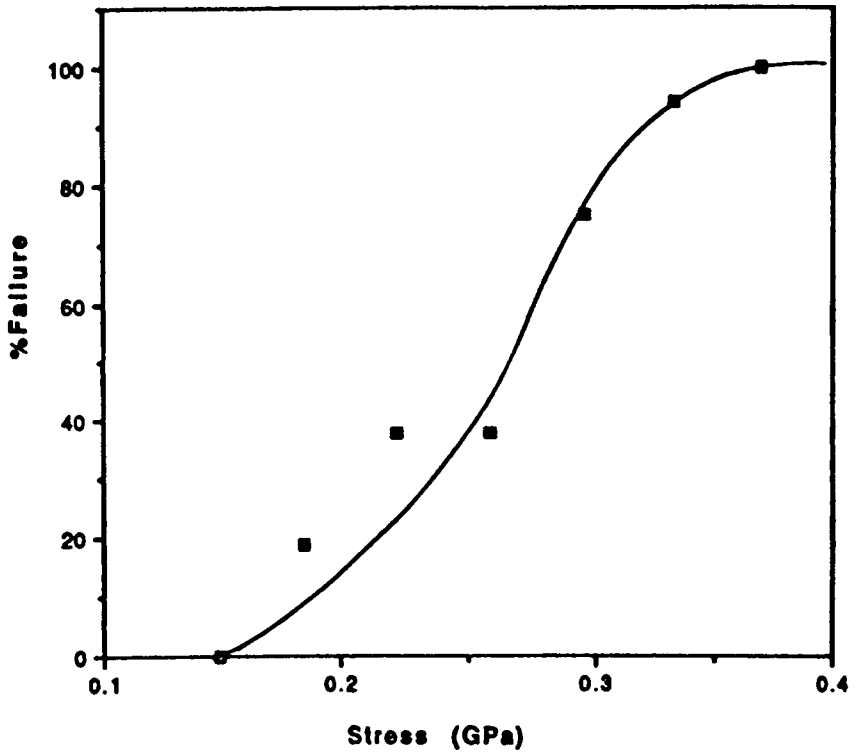


**Figure 7** Percent failure (fibers exhibiting kink) vs. recoil stress for PBZT fiber.

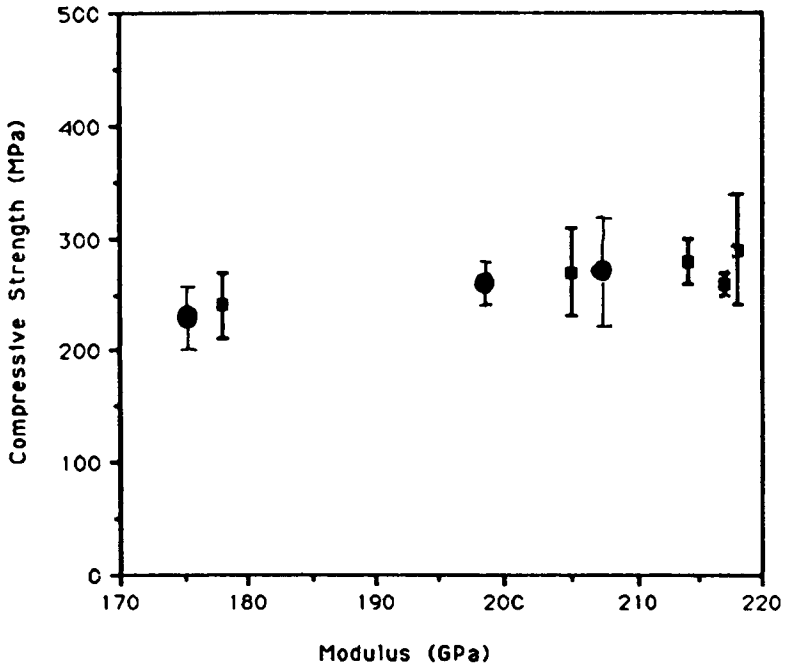


**Figure 8** Compressive strength vs. tensile modulus of PBZT fibers. (●) As-received fibers (heat treated below 700°C); (■) PBZT fiber F post heat treated at 725, 750, and 775°C.

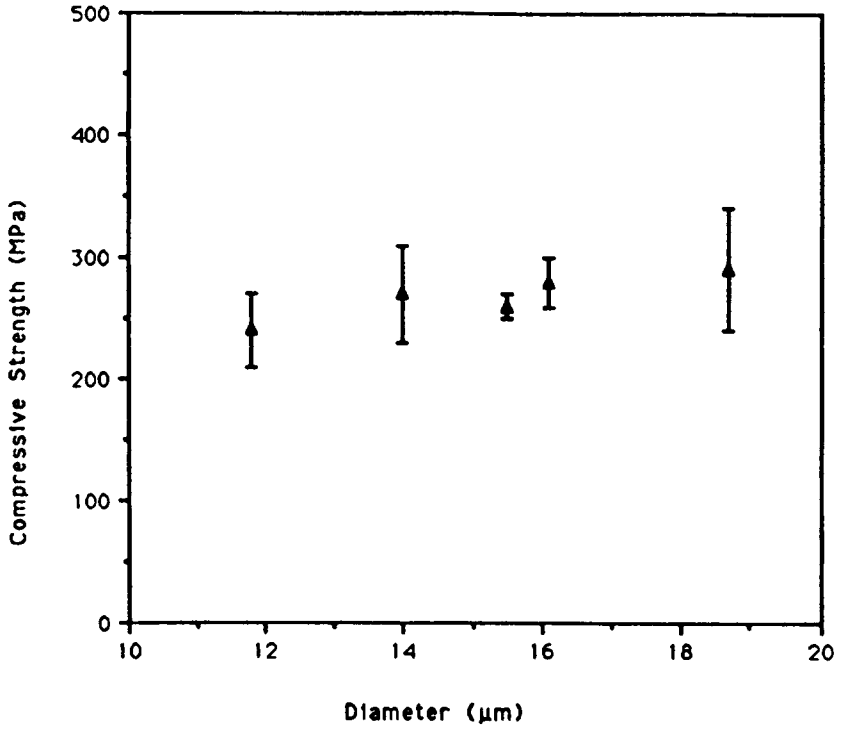


**Figure 9** PBZT fiber compressive strength as a function of fiber diameter.

scans where significantly reduced intensity is observed for the post heat-treated fibers as compared to the control sample (fiber F). This suggests increased order along the chain axis on post heat treatment. Based on these considerations it appears that the decrease in swelling may have been a result of increased order and crystallinity rather than significant crosslinking. Therefore it is not surprising that no increase in compressive strength was observed on post heat treatment. Attempts to chemically modify the polymer structure for the purpose of inducing crosslinking both in the rigid-rod polymer systems and in aramids have been reported. However the results of these attempts on compres-

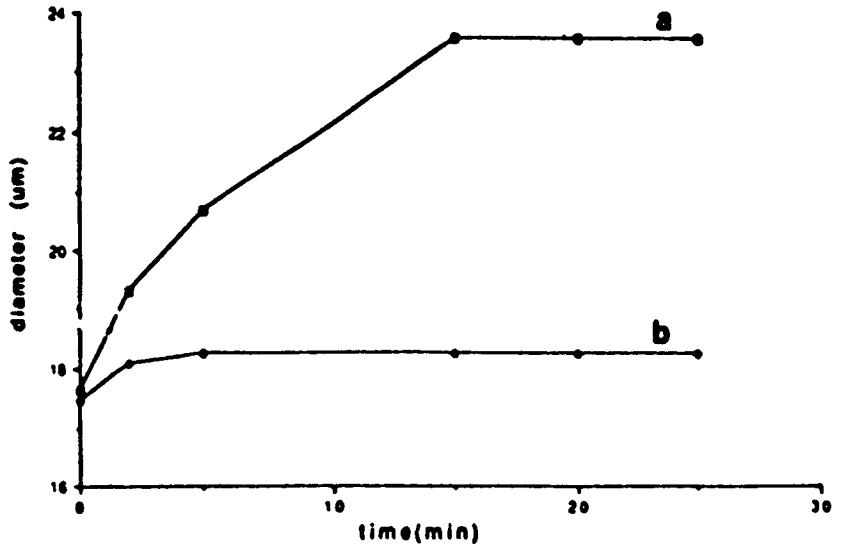


**Figure 10** PBZT fiber swelling. Fiber diameter as a function of time in 85% methane sulfonic acid. (a) As-received fiber F and (b) fiber F post heat treated at 725°C.

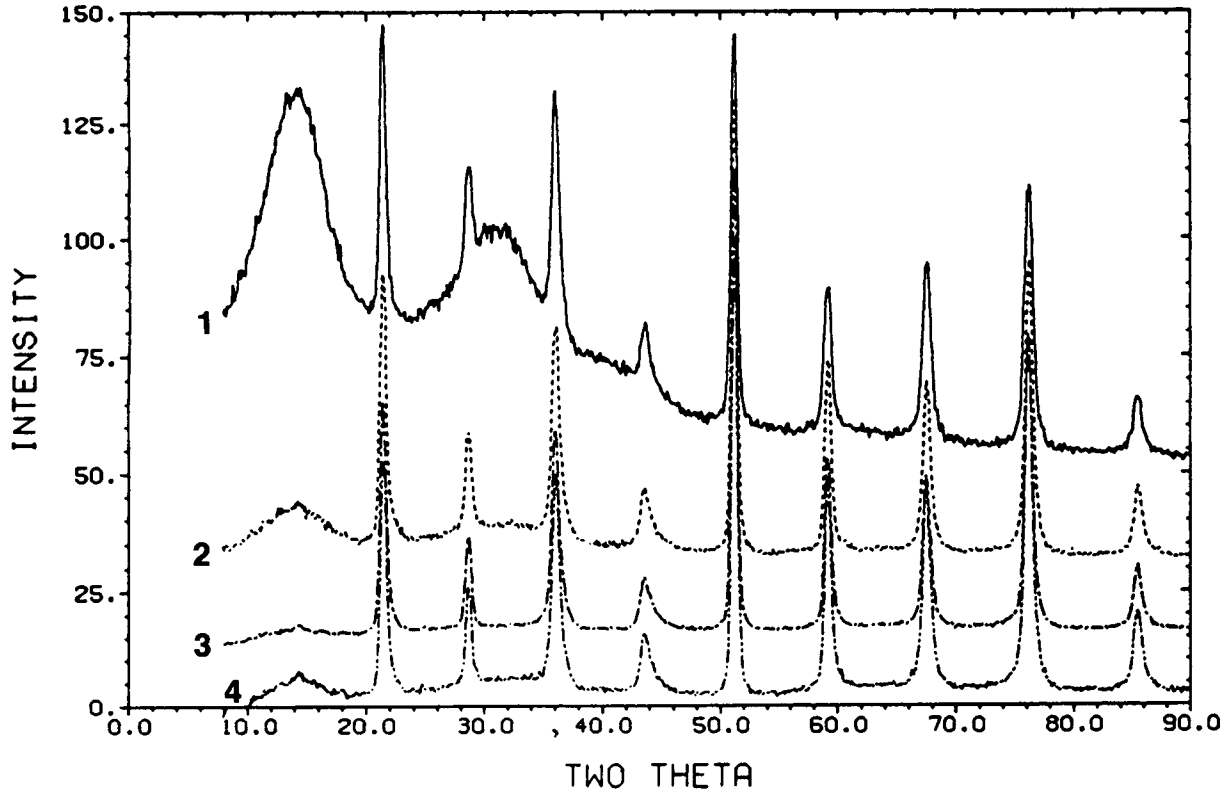


**Figure 11** Meridional radial x-ray scattering scans from PBZT fiber F (scan 1) and the fiber post heat treated at 725 (scan 2), 750 (scan 3), and 775°C (scan 4). Radiation used Cu K$\alpha$.

sive strength improvements have not been very encouraging and conclusive.[2,4,17-21] Fiber torsional modulus measured using torsional pendulum[22] for both the as-received and the post heat-treated fiber was 1.1 GPa. Small angle x-ray scattering of the post heat-treated fiber and that for the PBZT fiber F has an equatorial streak generally attributed to the voids elongated along the fiber axis. The post heat-treated fiber also has significant intensity around the meridian indicating the development of inhomogeneity in the fiber on post heat treatment. However the distinct four point scattering pattern observed in the poly(*p*-phenylene benzobisoxazole) fiber[23] is not observed in the post heat-treated PBZT fiber.

## SUMMARY

Compressive and tensile behavior of PBZT fibers was evaluated. PBZT fibers were characterized with two failure modes in tension. Mode I fibers with relatively higher average tensile strength exhibited little or no axial fiber splitting. Mode II with significant axial splitting has lower tensile strength. Fiber tensile behavior was analyzed using Weibull distribution. Fiber retains 80% of its room temperature tensile strength and modulus at 150°C. Fiber compressive strength was measured using the recoil test. No significant compressive strength dependence was observed either on modulus or on fiber diameter. Fiber post heat treatment between 725 and 775°C for 30 s resulted in reduced fiber swelling and enhanced crystallite size and higher order along the chain axis. No evidence of crosslinking was observed in the post heat-treated fibers using FTIR.

We are grateful to Dr. D. P. Anderson of the University of Dayton Research Institute (UDRI) for the x-ray scattering and to Gary Price of UDRI for the scanning electron microscopy of the kink bands.

## REFERENCES

1. N. Venkatasubramanian, M. B. Polk, S. Kumar, and L. T. Gelbaum, *J. Polym. Sci., Polym. Phys. Ed.*, **31**, 1965 (1993).

2. S. Kumar in *International Encyclopedia of Composites,* Vol. 4, S. M. Lee, Ed., VCH, New York, 1991, p. 51.
3. J. F. Wolfe in *Encyclopedia of Polymer Science and Engineering,* Wiley, New York, Vol. 11, 1988, p. 601.
4. W. W. Adams, R. K. Eby, and D. E. McLeMore, Eds., *The Materials Science and Engineering of Rigid-Rod Polymers,* MRS Symp. Proc., Pittsburgh, PA, 1989, p. 134.
5. V. V. Kozey and S. Kumar, *J. Mater. Res.,* **9,** 2717 (1994).
6. V. V. Kozey, H. Jiang, V. R. Mehta, and S. Kumar, *J. Mater. Res.,* **10,** (1995) in press.
7. V. V. Kozey and S. Kumar, to appear.
8. S. Allen, *J. Mater. Sci.,* **22,** 853 (1987).
9. M. Sahafeyan, M.S. thesis, Georgia Institute of Technology, Atlanta, GA, March 1993.
10. A. Crasto and S. Kumar, *SAMPE Proc.,* **35,** 318 (1990).
11. C. S. Wang, S. J. Bai, and B. P. Rice, *Polym. Mater. Sci. Eng. Prepr.* (ACS), **61,** 550 (1989).
12. A. J. Perry, B. Ineichen, and B. Eliasson, *J. Mater. Sci., Lett.,* **9,** 1376 (1974).
13. W. Weibull, *J. Appl. Mech.,* **18,** 293 (1951).
14. C. P. Beetz, Jr., *Fiber Sci. Technol.,* **16,** 45 (1982).
15. C. P. Beetz, Jr., *Fiber Sci. and Technol.,* **16,** 81 (1982).
16. R. J. Morgan, C. O. Pruneda, and W. J. Steele, *J. Polym. Sci., Poly. Phys. Ed.,* **21,** 1757 (1983).
17. S. Kumar and T. E. Helminiak, in *The Materials Science and Engineering, of Rigid-Rod Polymer,* W. W. Adams, R. K. Eby, and D. E. McLeMore, Eds., MRS Symp. Proc., Pittsburgh, PA, 1989 p. 364.
18. C. Rickert, P. Neuenschwander, and U. W. Suter, *Macromol. Chem. Phys.,* **195,** 511 (1994).
19. B. Glomm, C. Rickert, P. Neuenschwander, and U. W. Suter, *Macromol. Chem. Phys.,* **195,** 525 (1994).
20. W. Sweeny, *J. Polym. Sci., Polym. Chem. Ed.,* **30,** 1111 (1992).
21. D. C. Martin, T. Jiang, J. Rigney, M. C. Jones, L. Markoski, and J. S. Moore, *Polym. Prepr. (ACS),* **34,** 720 (1993).
22. V. R. Mehta and S. Kumar, *J. Mater. Sci.,* **29,** 3658 (1994).
23. S. Kumar, S. Warner, D. T. Grubb, and W. W. Adams, *Polymer,* **35,** 5408 (1994).

*Received July 31, 1994*
*Accepted November 1, 1994*